Dissipative Particle Dynamics Simulations of Polymer Chains: Scaling Laws and Shearing Response Compared to DNA Experiments

Vasileios Symeonidis,[1,*] George Em Karniadakis,[1,†] and Bruce Caswell[2,‡]
[1]*Division of Applied Mathematics, Brown University, Providence, Rhode Island 02912, USA*
[2]*Division of Engineering, Brown University, Providence, Rhode Island 02912, USA*

(Received 19 October 2004; revised manuscript received 28 June 2005; published 12 August 2005)

Dissipative particle dynamics simulations of several bead-spring representations of polymer chains in dilute solution are used to demonstrate the correct static scaling laws for the radius of gyration. Shear flow results for the wormlike chain simulating single DNA molecules compare well with average extensions from experiments, irrespective of the number of beads. However, coarse graining with more than a few beads degrades the agreement of the autocorrelation of the extension.

DOI: 10.1103/PhysRevLett.95.076001 PACS numbers: 83.10.Pp, 83.10.Rs, 83.50.Ax, 83.80.Rs

Modeling realistic polymer motion in the microscopic or mesoscopic level in equilibrium and simple flow configurations has been a continuous challenge in terms of (a) the choice of appropriate polymeric interactions and (b) the simulation method itself. Brownian dynamics (BD) simulations [1] have shown a good comparison [2] with experiments on DNA molecules in shear flow [3]. Molecular dynamics (MD) has been used for comparison with wormlike chain (WLC) [4] and slip length measurements for sheared films [5] but the number of beads and the time scale interval is much shorter than the times for gathering experimental data (of the order of seconds [3]). Here we employ dissipative particle dynamics [(DPD), described below] to investigate the static scaling law for several model chains and the response of the WLC under shear. This mesoscopic method has already been used to model macromolecules in a variety of equilibrium and nonequilibrium configurations [6–10].

In the motion of ideal chains, the bonds—characterized by linear elastic forces—are not restricted from passing through each other, crossings known as *phantom collisions*. For real chains in good solvents these unphysical collisions are eliminated by the constraint of self-avoiding walks on preset lattice paths. This dramatically affects their scaling properties. Our treatment of chains places no explicit constraints on the interaction between chain segments. Since it is usually assumed that in physical systems self-avoidance is a consequence of excluded volume and restricted bond rotation, we attempt to exclude phantom collisions by appropriate choices of *intrapolymer* interactions. Our chain potentials contain no angle dependence and therefore only the excluded volume is available for the task of self-avoidance. Since the detection of phantom collisions is computationally complex, their frequency is measured indirectly by checking the scaling exponents of the radius of gyration, R_g, with respect to chain size. For a chain of M beads it is defined by $\langle {R_g}^2 \rangle = \langle \frac{1}{M} \sum_{i=1}^{M} (R_i - R_{\mathrm{cm}})^2 \rangle$, where R_i is the position vector of each bead, R_{cm} the position vector of the center of mass of the chain, and $\langle * \rangle$ denotes time averaging. Statistical scaling arguments show that $R_g \propto (M-1)^{\nu}$. The static exponent ν is 0.5 for ideal chains (in any space dimension d [11]), and for real chains is $\nu = \frac{3}{d+2} = 0.6$ (Flory's formula), which has been verified by light scattering experiments [11]. Previous DPD simulations involved linear chains [6,7] and manipulation of solvent characteristics [8] to obtain the 0.6 exponent *without* appropriate interbead forces.

In 1992 Hoogerbrugge and Koelman [12] introduced the DPD method, which combines some of the detailed description of the MD with the ability to describe larger time and length scales. The DPD method describes *blocks* of molecules moving together in a coherent fashion subject to soft potentials and governed by predefined collision rules. Hence, this method is very attractive for the computer simulation of polymer solutions, since by employing the bead-spring model of polymer chains we can formulate and compare a variety of realistic conservative interbead forces. In contrast to Langevin-equation methods, such as BD, the hydrodynamic resistance is accounted for implicitly by the DPD solvent particles which behave as a Newtonian fluid [13].

As a particle-based mesoscopic method, DPD considers N particles, each having mass m_i, whose momenta and position vectors are governed by Newton's equations of motion. For a typical particle i, $\mathbf{v}_i = \frac{d\mathbf{r}_i}{dt}$, $\mathbf{F}_i = m_i \frac{d\mathbf{v}_i}{dt}$, where $\mathbf{v}_i$ its velocity, $\mathbf{r}_i$ its position, and $\mathbf{F}_i$ its net force. The interparticle force $\mathbf{F}_{ij}$ exerted on particle i by particle j is composed of conservative ($\mathbf{F}^c_{ij}$), dissipative ($\mathbf{F}^d_{ij}$), and random ($\mathbf{F}^r_{ij}$) components. Hence, the total force on particle i is given by $\mathbf{F}_i = \sum_{i \neq j} \mathbf{F}^c_{ij} + \mathbf{F}^d_{ij} + \frac{\mathbf{F}^r_{ij}}{\sqrt{\Delta t}}$, Δt being the simulation time step. The sum acts over all particles within a cutoff radius r_c beyond which the forces are considered negligible. We set the interaction radius to $r_c = 1$, thus defining the length scale of the system. Denoting $\mathbf{r}_{ij} = \mathbf{r}_i - \mathbf{r}_j$, $\mathbf{u}_{ij} = \mathbf{u}_i - \mathbf{u}_j$, $r_{ij} = |\mathbf{r}_{ij}|$, and the unit vector

$\mathbf{e}_{ij} = \frac{\mathbf{r}_{ij}}{r_{ij}}$, the forces are

$$\mathbf{F}^c_{ij} = F^{(c)}(r_{ij})\mathbf{e}_{ij}, \qquad \mathbf{F}^d_{ij} = -\gamma\omega^d(r_{ij})(\mathbf{u}_{ij}\cdot\mathbf{e}_{ij})\mathbf{e}_{ij},$$

$$\mathbf{F}^r_{ij} = \sigma\omega^r(r_{ij})\xi_{ij}\mathbf{e}_{ij},$$

where the ξ_{ij} are symmetric Gaussian random variables with zero mean and unit variance and σ, γ are coupled by $\sigma^2 = 2\gamma k_B T$, k_B being the Boltzmann constant and T the temperature of the system [14]. A common choice for the conservative force is a soft repulsion given by $F^{(c)}(r_{ij}) = a_{ij}\max\{1 - \frac{r_{ij}}{r_c}, 0\}$. The dissipative and random forces, on the other hand, are characterized by strengths $\omega^d(r_{ij})$ and $\omega^r(r_{ij})$ coupled by $\omega^d(r_{ij}) = [\omega^r(r_{ij})]^2 = \max\{(1 - \frac{r_{ij}}{r_c})^2, 0\}$. The above relation is necessary for thermodynamic equilibrium. The dissipative forces represent friction between the particles and account for energy loss, while the random ones compensate for lost degrees of freedom due to coarse graining and heat up the system.

The conservative forces present in the DPD equations can be tailored to describe a variety of interactions $F^{(c)}(r_{ij}) = \nabla V(r_{ij})$, for a potential V. In this work, polymers are chains of beads (DPD particles) subject to the standard DPD forces: soft repulsive (conservative), dissipative, and random. *In addition*, they are subject to intrapolymer forces arising from different combinations of the following types:

Lennard-Jones.—The force for each pair of bead particles is given by the shifted (to avoid numerical instabilities) LJ potential $U_{\mathrm{LJ}} = 4\epsilon[(\frac{L}{r_{ij}})^{12} - (\frac{L}{r_{ij}})^6 + \frac{1}{4}]$ truncated to act *only* for pairs with $r_{ij} < r_c$. We pick $\epsilon = k_B T$, $L = 2^{-1/6}$, and $r_c = L \times 2^{-1/6} = 1$. We note that the LJ potential used here is defined at the mesoscopic level to improve polymeric self-avoidance—softer repulsion rules [15] are an alternative.

Hookean and Fraenkel.—The interbead force is derived from a pairwise potential with equilibrium length r_{eq}. Since the force is proportional to $[|\mathbf{r}_i - \mathbf{r}_{i-1}| - r_{\mathrm{eq}}]$, it is attractive or repulsive depending if $|\mathbf{r}_i - \mathbf{r}_{i-1}| >$ or $< r_{\mathrm{eq}}$. As $r_{\mathrm{eq}} \to 0$ we recover the Hookean spring.

FENE.—The finitely extensible nonlinear elastic (FENE) spring has a maximum bond extension $r_{\max}$ beyond which the force becomes infinite, and hence any length greater than $r_{\max}$ is not allowed. The potential for M beads is described by $U_{\mathrm{FENE}} = -\frac{\kappa}{2} r^2_{\max} \log[1 - \frac{|\mathbf{r}_i - \mathbf{r}_{i-1}|^2}{r^2_{\max}}]$.

Wormlike chain (WLC).—The Marko-Siggia (M-S) [16] force expression $\frac{k_B T}{\lambda_p}[\frac{1}{4(1-R)^2} - \frac{1}{4} + R]$, where λ_p is the persistence length, L_{sp} is the maximum length of the spring, and $R = \frac{|\vec{r}_i - \vec{r}_{i-1}|}{L_{\mathrm{sp}}}$. For chains with more than 2 beads, λ_p was adjusted using the analysis and results presented in [17].

In the above, κ is the spring constant, $i = 2, \ldots, M$, and the interbead force in each case is $\mathbf{F}^p = -\nabla U$.

Single chains immersed in "an ocean" of DPD particles constitutes a mesoscopic model of a dilute polymer solution. Hence, the dynamics of a single flexible polymer chain is of great importance for validation and physical understanding of the method. Our work introduces combinations of forces aiming to illustrate excluded volume effects and phantom collision minimization (well documented with other methods), *not* through immiscibility of the solvent but through different bead-spring representations. Figure 1 summarizes results for different spring laws with and without bead-bead repulsions. The corresponding static exponent values (ν) of the radius of gyration are computed for each case, using 5-, 10-, 20-, 50-, and 100-bead chains. The LJ repulsion seems to be mostly responsible for capturing *self-avoidance* while the underlying spring force (Hookean or FENE) appears to have a secondary effect on the scaling exponent, when coupled with hard repulsions. However, FENE forces alone scale close to the Flory exponent, rendering the model realistic without any additional repulsions. The FENE parameter $r_{\max}$ was also varied, with the values $2r_c$ and $3r_c$ giving very similar scaling laws (Fig. 1). The parameters for the WLC were consistent with the rest of the models [18].

DNA molecules under steady shear have been extensively studied in experimental [3] and computational [2,15] works. Using DPD we investigated the dynamics of a single WLC. The moving boundaries at $y = 0$, $y = L_y$ are modeled using Lees-Edwards boundary conditions [19]: particles leaving the domain at $y = 0$, L_y are advanced or retarded by an increment of $\Delta r = U_x t$, $-U_x t$, respectively, in the x direction, where t is the time elapsed from an appropriate origin of times and U_x denotes twice

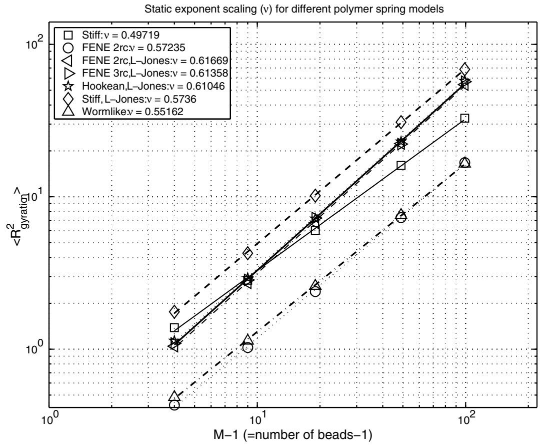

FIG. 1. Scaling of the radius of gyration of a single polymer chain governed by linear, WLC, and FENE forces and the effect of hard LJ potentials. The chain sizes vary from 5 to 100 beads, with $r_{\max} = 2r_c, 3r_c$, $\kappa = \frac{1}{\lambda_p} = 7$, $r_{\mathrm{eq}} = r_c$, $L_{\mathrm{sp}} = 2r_c$. Integration time is 10 000 units with time step $\Delta t = 0.01$.

the shear velocity of each boundary. Moreover, the velocity of the particle is increased or decreased by U_x, $-U_x$, accounting for both the imposed boundary condition and the velocity discontinuity between the two walls. The rest of the boundaries are treated periodically for all the solvent DPD particles. To avoid unphysical periodicity artifacts, polymer beads *only* undergo an elastic collision in the y direction: $(u, v, w)_{\mathrm{BEAD}} \rightarrow (u, -v, w)_{\mathrm{BEAD}}$ and $r_y \rightarrow r_y - (\Delta t) v_{\mathrm{BEAD}}$. Different chain sizes were accommodated by storing the polymer coordinates without mapping them back in the original domain. This allowed the intrapolymer forces to be calculated properly, while the collective solvent-solvent and polymer-solvent interactions were calculated with the mapped (periodic) images. The effect of the simulation box size $L_x \times L_y \times L_z$ for the presented results was investigated and proved to be negligible.

WLC parameters for stained λ-phage DNA were assumed to have $L = 21.1$ μm (fully extended length) and $\lambda_p = 0.053$ μm (persistence length). In DPD units we fixed $L = 42.2 r_c$, $\lambda_p = 0.106 r_c$, and $k_B T = 0.2$. For a M-bead chain ($M = 2, 5, 10, 20$), therefore, $L_{\mathrm{sp}} = \frac{42.2}{M-1}$. The calculated mean-square extension of an initially 30%-extended chain was fitted with $\langle x^2 \rangle = \langle x^2 \rangle_0 + x_i^2 e^{-t/\tau}$ to obtain the chain relaxation time τ, and hence the Weissenberg number $\mathrm{We} = \dot{\gamma}\tau$, for a shear rate $\dot{\gamma}$. Figure 2 shows the calculated average molecular (maximum projected) extension and the experimental data [3] versus We, with varying bead numbers and corresponding relaxation times. The asymptotic value for 20 beads ($\approx$0.51) is in agreement with the corresponding one (0.47) from BD calculations [2]. Remarkably, the results for the average extension are not so sensitive to coarse graining, i.e., the number of beads used for constant L, in the tested range. The self-consistency of the parameters was verified from the equilibrium mean-square end-to-end distance of a 2-bead dumbbell, computed as $\langle S^2 \rangle \approx 8.56$, in close agreement with the theoretical value of 8.92 given by [20] $\langle S^2 \rangle = 2 L_{\mathrm{sp}} \lambda_p [1 - \frac{\lambda_p}{L_{\mathrm{sp}}}(1 - e^{-L_{\mathrm{sp}}/\lambda_p})]$. While most results presented in this work employ the widely used velocity-Verlet scheme for time integration, in Fig. 2 we have also included results for 2 beads using Lowe's method [21], a different DPD approach coupling MD with an Andersen thermostat. Figure 3 compares the calculated [22] normalized autocorrelation function $\langle \Delta x(t) \Delta x(t + T) \rangle$, $\Delta x(t) = x(t) - \langle x(t) \rangle$ for 2-, 5-, and 20-bead chains, with experimental data [3]. It demonstrates the sensitivity of the autocorrelation to coarse graining of the M-S force-extension formula. Significant degradation in the agreement with experiments appears for more than 5 beads. This shows the limits of the coarse graining of a mesoscopic relation such as M-S. The M-S formula gives the average end force of a chain consisting of a large number of microelements (bead rods freely rotating at fixed bond angles). The coarse grained counterparts of the M-S chains rotate about their beads with any bond angle. We have compensated for this freedom by altering λ_p in the M-S formula for the subchains in the spirit of [17]. Clearly, a 2-bead dumbbell cannot describe the instantaneous configurations of DNA observed by [3]. If their capture is the objective of simulation, then the model needs to consist of a large number of microelements such as the 220 freely rotating, bead-rod chains of [2]. With fixed bond angle these become the microelements of the WLC, widely considered to be an appropriate model for DNA. To date, their simulation has yet to be attempted.

Finally, we map the computed results, which are in DPD reduced units, into dimensional units. In our DPD simulations, a single WLC represents a λ-phage DNA molecule, with a static end-to-end distance of $S \approx 3.5$ μm. Denoting all scaling factors by $[*]$, we find the average end-to-end distance (20 beads) through an equilibrium simulation to be $3.95[r_c]$. Hence, $3.95[r_c] = S \approx 3.5 \times 10^{-6}$ m or $[r_c] \approx 0.89 \times 10^{-6}$ m. The volume of one cell in the domain is $[r_c]^3 \approx 7.05 \times 10^{-19}$ m^3 and since the density

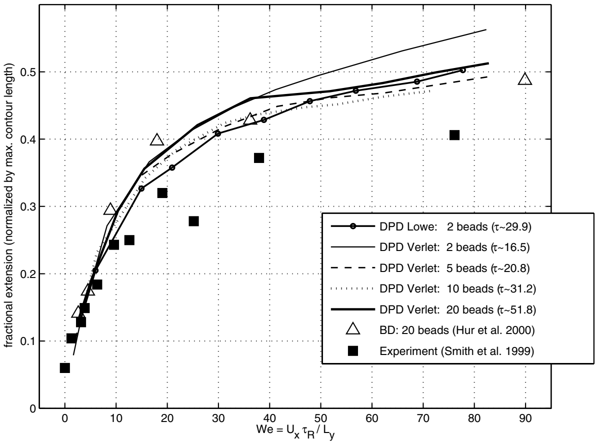

FIG. 2. Mean WLC fractional extension versus We compared to BD [2] and DNA experiments [3] data.

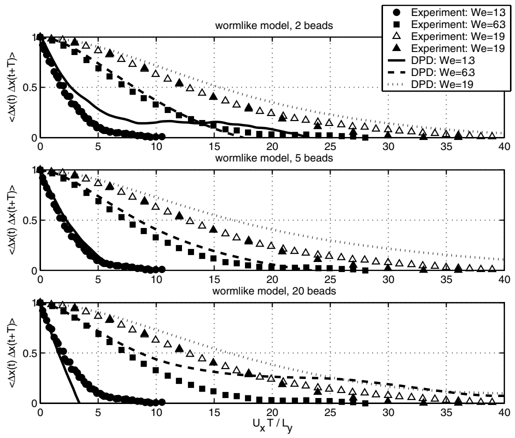

FIG. 3. Autocorrelation of molecular extension x vs $\dot{\gamma}T$, compared with experimental DNA [3] data, for various We.

ρ is taken to be 4 throughout, we compute the density scaling (for water solvents) to be $[\rho] = \frac{1}{4} \times 997\ \mathrm{kg/m^3} = 249.25\ \mathrm{kg/m^3}$ at $T = 25\,^\circ\mathrm{C}$. Hence, the corresponding mass of each particle (each cell contains 4 particles on average) is given by $[\mathrm{m}] \approx 249.25 \times 7.05 \times 10^{-19}\ \mathrm{kg} = 1.76 \times 10^{-16}$ kg. Next, we use the thermal velocity given by $V_{\mathrm{rms}} = \sqrt{3k_B T/\mathrm{m}}$, where $k_B = 1.38 \times 10^{-23}$ J/K and $T = 298$ K to find the time units based on the *solvent* motion: $[V]_s \approx 0.0084\ \frac{\mathrm{m}}{\mathrm{s}}$ and therefore $[t]_s = \frac{[r_c]}{[V]} \approx \frac{0.89\times 10^{-6}\ \mathrm{m}}{0.0084\ \mathrm{m/s}} = 1.06 \times 10^{-4}$ s. Our DPD time step is $\Delta t = 0.02$, a physical time of $\Delta t = 2.12 \times 10^{-6}$ s. For reaching a solution time of 10 000 units, our total integrating time is $500\,000 \times \Delta t \approx 1.06$ s. The solvent-based computational time compares well with DNA experimental statistics gathered over seconds. However, the slower dynamics of the *polymer* units yield markedly larger time scales. We take a typical polymer relaxation time $\tau \approx 51.8$ (20 beads) which gives $[t]_p = \frac{6.3}{51.8}\ \mathrm{s} \approx 0.12$ s. The close agreement with BD simulations [2] and the experimental data [3] suggests these scales to be appropriate. Moreover, the shear velocity range for a length $L_y = 20[r_c]$ spans the interval $[1, 32]$ in DPD units, which scales to $[r_c] \times [1, 32]/[t]_p \approx [7, 237]\ \frac{\mu\mathrm{m}}{\mathrm{s}}$, within reasonable agreement with the values $[10, 200]\ \frac{\mu\mathrm{m}}{\mathrm{s}}$ used in [3].

The authors would like to acknowledge the support of NSF/CTS and NSF/ITR.

---

*Electronic address: sjoh0341@dam.brown.edu
†Electronic address: gk@dam.brown.edu
‡Electronic address: caswell@dam.brown.edu

[1] P. S. Doyle and E. S. G. Shaqfeh, J. Non-Newtonian Fluid Mech. **76**, 43 (1998).
[2] J. S. Hur, E. S. G. Shaqfeh, and R. G. Larson, J. Rheol. (N.Y.) **44**, 713 (2000).
[3] D. E. Smith, H. P. Babcock, and S. Chu, Science **283**, 1724 (1999).
[4] M. Cheon, I. Chang, J. Koplik, and J. R. Banavar, Europhys. Lett. **58**, 215 (2002).
[5] N. V. Priezjev and S. M. Troian, Phys. Rev. Lett. **92**, 018302 (2004).
[6] A. G. Schlijper, P. J. Hoogerbrugge, and C. W. Manke, J. Rheol. (N.Y.) **39**, 567 (1995).
[7] N. A. Spenley, Europhys. Lett. **49**, 534 (2000).
[8] Y. Kong, C. W. Manke, W. G. Maddenand, and A. G. Schlijper, J. Chem. Phys. **107**, 592 (1997).
[9] C. M. Wijmans and B. Smit, Macromolecules **35**, 7138 (2002).
[10] S. Chen, N. Phan-Thien, X.-J. Fan, and B. C. Khoo, J. Non-Newtonian Fluid Mech. **118**, 65 (2004).
[11] P.-G. de Gennes, *Scaling Concepts in Polymer Physics* (Cornell University Press, Ithaca, 1979).
[12] P. J. Hoogerbrugge and J. M. V. A. Koelman, Europhys. Lett. **19**, 155 (1992).
[13] R. D. Groot, T. J. Madden, and D. J. Tildesley, J. Chem. Phys. **110**, 9739 (1999).
[14] P. Español and P. Warren, Europhys. Lett. **30**, 191 (1995).
[15] R. M. Jendrejack, J. J. de Pablo, and M. D. Graham, J. Chem. Phys. **116**, 7752 (2002).
[16] J. F. Marko and E. D. Siggia, Macromolecules **28**, 8759 (1995).
[17] P. T. Underhill and P. S. Doyle, J. Non-Newtonian Fluid Mech. **122**, 3 (2004).
[18] Different parameters, taken from DNA molecules, produced $\nu = \frac{1}{2}$—indicative that the DNA-wormlike model in equilibrium operates mostly in the linear regime.
[19] A. W. Lees and S. F. Edwards, J. Phys. C **5**, 1921 (1972).
[20] S. F. Sun, *Physical Chemistry of Macromolecules* (Wiley, New York, 1994).
[21] C. P. Lowe, Europhys. Lett. **47**, 145 (1999).
[22] The products for each pair were collected from single-chain simulations in time bins with $\frac{\tau[\mathrm{DPD}]}{\tau[\mathrm{EXP}]} \times \frac{1}{\Delta t}$ sample points, $\tau[\mathrm{DPD}]$ being the longest relaxation time in DPD units for each case, $\tau[\mathrm{EXP}]$ typically fixed to 6.3, and Δt the simulation time step, as done in [3].